# Unusual Iron(III) Ate Complexes Stabilized By Li – π Interactions

**Garry Mund,[a] Dragoslav Vidovic,[a] Raymond J. Batchelor,[a] James F. Britten,[b]
Rajendra D. Sharma,[a] Colin H. W. Jones,[a] and Daniel B. Leznoff*[a]**

**Abstract:** Several iron(III) complexes incorporating diamidoether ligands are described. The reaction between $\{Li_2[RN(SiMe_2)]_2O\}$ and $FeX_3$ (X = Cl or Br; R = 2,4,6-Me$_3$Ph or 2,6-$i$Pr$_2$Ph) form unusual ate complexes, $\{FeX_2Li[RN(SiMe_2)]_2O\}_2$ (**2**, X = Cl, R = 2,4,6-Me$_3$Ph; **3**, X = Br, R = 2,4,6-Me$_3$Ph; **4**, X = Cl, R = 2,6-$i$Pr$_2$Ph) which are stabilized by Li – π interactions. These dimeric iron(III) – diamido complexes exhibit magnetic behaviour characteristic of uncoupled high spin ($S = 5/2$) iron(III) centres. They also undergo halide metathesis resulting in reduced iron(II) species. Thus, reaction of **2** with alkyllithium reagents leads to the formation of iron(II) dimer $\{Fe[Me_3PhN(SiMe_2)]_2O\}_2$ (**6**). Similarly, the previously reported iron(III) – diamido complex $\{FeCl[tBuN(SiMe_2)]_2O\}_2$ (**1**) reacts with $LiPPh_2$ to yield the iron(II) dimer $\{Fe[tBuN(SiMe_2)]_2O\}_2$ but reaction with $LiNPh_2$ gives the iron(II) product $\{Fe_2(NPh_2)_2[tBuN(SiMe_2)]_2O\}$ (**5**). Some redox chemistry is also observed as side reactions in the syntheses of **2** – **4**, yielding THF adducts of $FeX_2$: the one-dimensional chain $[FeBr_2(THF)_2]_n$ (**7**) and the cluster $[Fe_4Cl_8(THF)_6]$. The X-ray crystal structures of **3**, **5** and **7** are described.

**Keywords:** ate complexes · diamido ligands · iron · magnetic properties · Moessbauer spectroscopy

## Introduction

Amido donors are versatile ligands due to their ease of steric and electronic modification (via the nitrogen substituent) and are ideal for the stabilization of high-oxidation state metal centres due to their strong π-donating ability.[1] In particular, multidentate amido ligands have been shown to be excellent for the stabilization of high-valent diamagnetic organometallic systems, such as for Zr$^{IV}$ and Ti$^{IV}$-based alkene polymerization catalysts.[2–4] However, chelating diamido ligands have rarely been used with paramagnetic first-row transition metals[5–8] despite the expectation of very different chemistry compared with the classical monodentate $M[NR_2]_x$ system.[9–11] We herein report a series of unusual dinuclear diamido iron(III) ate complexes stabilized by Li – π interactions that have very different Mössbauer and magnetic properties when compared to the related lithium-free complexes that were recently reported.[12] As seen in the literature, ate complexes are not observed often in late transition-metal chemistry.[13] Although the suffix "ate" has been applied to many polyatomic anions in inorganic nomenclature (e.g. $[Zn(OH)_4]^{2-}$, tetrahydroxozinc*ate*(II))[14] the term ate has also more specifically been used to describe complexes that retain MX (M = alkali metal, X = halide) in metathesis reactions involving alkali metal salts and metal halides. Most of the reported examples of ate complexes contain lanthanides,[15–17] actinides[15, 18] or early transition metals.[16, 19]

## Results and Discussion

**Synthesis and structure of the ate complexes**: The reaction of $FeX_3$ with $Li_2[^RNON]$[8] gives ate complexes of the general formula $\{FeX_2Li[RN(SiMe_2)]_2O\}_2$ (**2**, X = Cl, R = 2,4,6-Me$_3$Ph; **3**, X = Br, R = 2,4,6-Me$_3$Ph; **4**, X = Cl, R = 2,6-$i$Pr$_2$Ph), which are soluble in hexanes. The $^1$H NMR spectra of all reported iron(III) complexes have broad, shifted peaks consistent with their paramagnetism. The UV/Vis spectra of **2** – **4** show an absorption band (likely LMCT) that shifts towards higher energy with chloride to bromide substitution (Table 1). The single crystal X-ray structure of **3** reveals a dimeric ate complex which is shown in Figure 1 with selected interatomic distances and bond angles detailed in Table 2; the X-ray structure of **4** is very similar. The unusual core of the structure consists of two iron atoms, four halides and two lithium atoms, the latter of which are stabilized by Li – π interactions via the aryl rings on the amido groups. The Li1−C distances of 2.481(9) – 2.532(11) Å and short Li1−Ct distance

---

[a] Prof. D. B. Leznoff, G. Mund, D. Vidovic, Dr. R. J. Batchelor,
Dr. R. D. Sharma, Prof. C. H. W. Jones
Department of Chemistry, Simon Fraser University
8888 University Drive, Burnaby, BC V5A 1S6 (Canada)
Fax: (+1)-604-291-3765
E-mail: dleznoff@sfu.ca

[b] Dr. J. F. Britten
Department of Chemistry, McMaster University
Hamilton, ON, L8S 4M1 (Canada)

DOI: 10.1002/chem.200305014

Table 1. Room temperature magnetic moments per iron centre, Mössbauer parameters (and error values) at 4.2 K and visible absorption bands for **1**–**5**.

| Compound | $\mu_{eff}$ B.M. | $\Delta E_Q$ [mm s$^{-1}$] | $\delta$ [mm s$^{-1}$] | UV/Vis [nm] ($\varepsilon$, M$^{-1}$ cm$^{-1}$) |
|---|---|---|---|---|
| $\{FeCl[tBuN(SiMe_2)]_2O\}_2$ (**1**) | 4.5 | 3.52(2) | +0.25(2) | 484 (4060) |
| $\{FeCl_2Li[Me_3PhN(SiMe_2)]_2O\}_2$ (**2**) | 5.9 | 1.72(3) | +0.32(3) | 508 (2700) |
| $\{FeBr_2Li[Me_3PhN(SiMe_2)]_2O\}_2$ (**3**) | 6.1 | 1.72(5) | +0.28(5) | 414 (1980) |
| $\{FeCl_2Li[iPr_2PhN(SiMe_2)]_2O\}_2$ (**4**) | 6.2 | 1.82(4) | +0.27(4) | 410 (3400) |
| $\{Fe_2(NPh_2)_2[tBuN(SiMe_2)]_2O\}$ (**5**) | 4.5 | 1.36(5) | +0.70(5) | 530 (1100) |

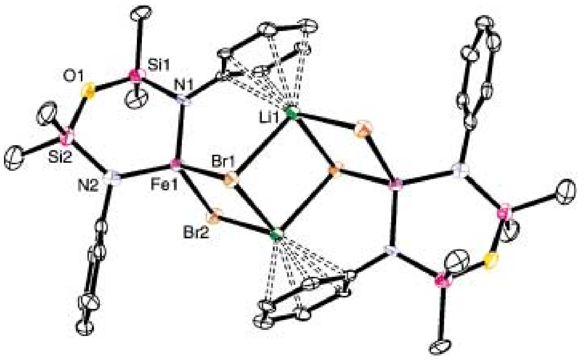

Figure 1. Molecular structure of **3** (ORTEP view, 33% probability ellipsoids are shown; methyl groups on aryl ring excluded for clarity).

Table 2. Selected interatomic distances [Å] and bond angles [°] for $\{FeBr_2Li[Me_3PhN(SiMe_2)]_2O\}_2$ (**3**).

| | | | |
|---|---|---|---|
| Fe1–N1 | 1.905(4) | Si1–O1 | 1.625(4) |
| Fe1–N2 | 1.877(5) | Si2–O1 | 1.632(4) |
| Fe1–Br1 | 2.4601(11) | N2-Fe1-N1 | 108.1(2) |
| Fe1–Br2 | 2.4313(11) | N2-Fe1-Br2 | 112.44(10) |
| Fe–Fe | 6.251 | N1-Fe1-Br2 | 114.47(12) |
| Fe1–O1 | 3.330 | N2-Fe1-Br1 | 117.11(12) |
| Si1–N1 | 1.734(5) | N1-Fe1-Br1 | 107.01(13) |
| Si2–N2 | 1.737(5) | Br2-Fe1-Br1 | 97.54(4) |
| | | Si1-O1-Si2 | 138.9(3) |

of 2.077 Å (Ct = centre of aromatic ring) in **3** are indicative of $\eta^6$-coordination.[20] This significant interaction may facilitate the formation of the ate complexes. The iron(III) centres have a pseudotetrahedral geometry; each is coordinated to two amido and two bridging halide ligands. The Fe–N distances of 1.877(5) and 1.905(4) Å are shorter than the 1.918(4) Å found in trigonal-planar $Fe[N(SiMe_3)_2]_3$,[10] or the 1.951(6) Å in trigonal bipyramidal $FeBr_2[N(SiMe_2CH_2PPh_2)_2]$.[21] The Fe–O distance of 3.330 Å in **3** is much longer than that observed in previously reported $\{FeCl[tBuN(SiMe_2)]_2O\}_2$ (**1**) (Fe–O: 2.597(4) Å), thus precluding any interaction between the ether donor of the ligand backbone and the corresponding iron atom.

**Magnetic properties of 2–4**: The temperature ($T$) dependence of the magnetic susceptibility ($\chi_M$) of **2**–**4** were measured on crystalline samples from 2 to 300 K (Table 1). The $\mu_{eff}$ vs $T$ plot for **2** is shown in Figure 2. The room temperature $\mu_{eff}$ value of 5.9 BM per iron atom agrees well with the spin-only value for five unpaired electrons (5.92 BM). The $\mu_{eff}$ values of **2**–**4** are essentially temperature independent until approximately 20 K, indicative of minimal coupling between the iron atoms of the dimer (Fe–Fe 6.251 Å in **3**). Below 20 K, **2**–**4** show zero-field splitting effects which cause a drop in the magnetic moment.[22] Hence, these ate complexes are examples of molecular high-spin tetrahedral iron(III) systems. There are noticeably few tetrahedral iron(III) complexes in the literature. $[FeI([D_5]pyridine)(N\text{-}RAr_f)_2]$ ($R = C(CD_3)_2CH_3$, $Ar_f = 2,5\text{-}C_6H_3FMe$)[23] and the thiourea iron(III) iodide complex $FeI_3[SC(NMe_2)_2]$[24] are two other examples. However, a large number of systems containing the high-spin, tetrahedral $[FeX_4]^-$ anion are well known.[25, 26] This geometry and spin state is also prominent in many solid-state[27] and bioinorganic systems.[28]

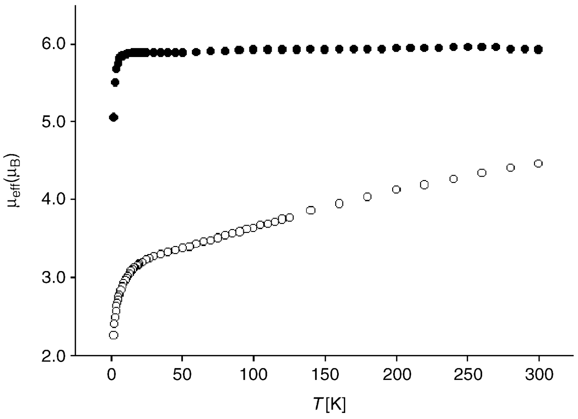

Figure 2. Plot of magnetic moment ($\mu_{eff}$) per iron vs temperature (K) for $\{FeCl_2Li[Me_3PhN(SiMe_2)]_2O\}_2$ (**2**; ●) and $\{Fe_2(NPh_2)_2[tBuN(SiMe_2)]_2O\}$ (**5**; ○).

The most relevant comparison to this series of ate complexes is the spin-admixed non-ate dimeric iron(III) complex **1**.[12] Spin admixture is a rare form of magnetic behaviour in which there is a quantum mechanical mixing of the $S = 5/2$ and $S = 3/2$ spin states through spin-orbit coupling, generating a new discrete spin state.[29] Presumably, the reason for the formation of the ate complexes **2**–**4** are the Li–π interactions that become available only when the *tert*-butyl groups are replaced by aromatic aryl groups on the amido donor. As a result, **1** is structurally quite different than the ate complexes. Since LiCl is retained in **2**–**4** and is included as part of the bridge between iron atoms, the Fe–Fe distance is very long compared to **1** (6.251 Å in **3** vs 3.4784(20) Å in **1**). This is reflected in the fact that the $\mu_{eff}$ of **1** drops significantly from 4.5 BM at 300 K to 3.0 BM at 50 K (indicative of antiferromagnetic coupling between the iron atoms of the dimer), while **2**–**4** show temperature independent behaviour throughout this temperature region. Furthermore, the ate complexes exhibit a pseudotetrahedral geometry about the iron atoms, with effective $C_{2v}$ symmetry, whereas the iron(III) centres in **1** have a distorted trigonal bipyramidal geometry and display much lower symmetry. In addition, the oxygen atom of the ligand backbone in **1** is weakly bound to the iron centres whereas in **2**–**4** no such interaction exists.

**Mössbauer spectra**: The Mössbauer spectra of **2**–**4** were measured on crystalline samples at 4.2 K. The Mössbauer spectrum of **2** is shown in Figure 3 and the Mössbauer parameters of **1**–**4** are shown in Table 1. Iron(III) complexes are usually characterized by small positive isomer shifts, with high spin complexes showing small (or even zero) quadrupole splittings.[30] The isomer shift ($\delta$) of **3** is $+0.28 \pm 0.05$ mm s$^{-1}$ (vs $\alpha$-Fe foil), consistent with an iron(III) centre (Table 1).[26, 31] The $\Delta E_Q$ of $1.72 \pm 0.05$ mm s$^{-1}$ observed in **3** is much larger than the values normally seen for tetrahedral high spin iron(III).[26] This is likely due to the considerable distortion from cubic symmetry in **2**–**4** ($C_{2v}$ vs $T_d$), thereby producing an electric field gradient at the iron atom. For comparison, both $[Et_4N]^+[FeX_4]^-$ and $[Et_4N]^+[FeCl_2Br_2]^-$ show a single line resonance at 77 K. Despite the non-cubic symmetry ($C_{2v}$) about the iron atom in the latter,[32] the minor difference in bonding between the chloride and bromide is not sufficient to generate a significant gradient whereas in **2**–**4** there is a considerable difference in bonding between the halide and amide.

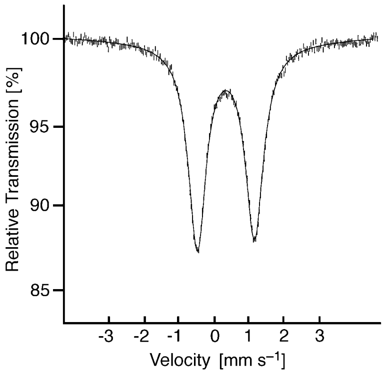

Figure 3. Mössbauer spectrum of **2** at 4.2 K.

However, **2**–**4** still show significantly smaller quadrupole splittings than the characteristically extremely large[33] $\Delta E_Q$ observed for spin-admixed **1** ($\Delta E_Q = 3.52 \pm 0.02$ mm s$^{-1}$).[12] The structural differences described above between **1** and **2**–**4** can account for the different spin states observed. The four-coordinate, pseudotetrahedral geometry of the ate complexes leads to pure high-spin ($S = 5/2$) systems as spin admixture cannot occur, whereas the five-coordinate trigonal bipyramidal geometry of **1** permits the deviation from an $S = 5/2$ state and subsequently results in spin-admixture.

**Reaction of 1 with LiNPh$_2$ and LiPPh$_2$**: Preliminary reactions indicate that both ate and non-ate iron(III) diamidoether complexes are reactive towards halide metathesis but often with unusual consequences. The reaction of non-ate **1** with LiNPh$_2$ resulted in halide substitution and concomitant generation of LiCl, however, a reduced iron(II) species was found to be the final product. The crystal structure of dimeric $\{Fe_2(NPh_2)_2[t\text{BuN}(SiMe_2)]_2O\}$ (**5**) is shown in Figure 4 with selected interatomic distances and bond angles in Table 3. The iron atoms are each bound to the two amido groups of the diamidoether ligand and the -NPh$_2$ group. The bridging Fe–N distances range from 2.042(2) to 2.072(2) Å and are comparable to those found in the iron(II)–amido complex $\{Fe[t\text{BuN}(SiMe_2)]_2O\}_2$.[5] However, in **5** the iron centres are bridged by only *one* diamidoether ligand—the reduction of Fe$^{III}$ to Fe$^{II}$ most likely results in the oxidation of the other diamidoether ligand from **1**. The Fe1–Fe2 distance of 2.5795(6) Å is shorter than in the structurally related $[Fe(NR_2)_2]_2$ complexes (2.663 Å, R = SiMe$_3$; 2.715 Å, R = Ph) possibly due to the chelating or less steric nature of the ligand.[11] The oxygen atom of the ligand backbone is associated with only one of the iron atoms (Fe1–O1 3.188(2) Å, Fe2–O1 2.587(2) Å).

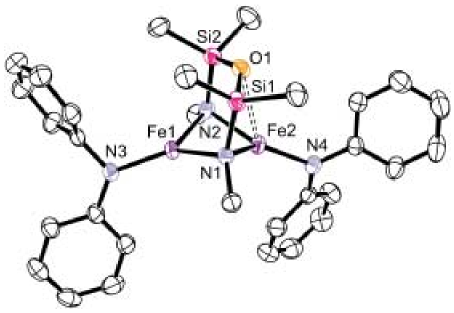

Figure 4. Molecular structure of **5** (ORTEP view, 50% probability ellipsoids are shown; *tert*-butyl groups simplified for clarity).

Table 3. Selected interatomic distances [Å] and bond angles [°] for $\{Fe_2(NPh_2)_2[t\text{BuN}(SiMe_2)]_2O\}$ (**5**).

| | | | |
|---|---|---|---|
| Fe1–Fe2 | 2.5795(6) | Si1–O1 | 1.645(2) |
| Fe2–O1 | 2.587(2) | Si2–O1 | 1.650(2) |
| Fe1–N1 | 2.059(2) | N1-Fe1-N2 | 95.21(9) |
| Fe1–N2 | 2.064(2) | N1-Fe2-N2 | 95.48(9) |
| Fe2–N1 | 2.072(2) | N1-Fe1-N3 | 136.7(1) |
| Fe2–N2 | 2.042(2) | N2-Fe1-N3 | 128.1(1) |
| Fe1–N3 | 1.926(2) | N1-Fe2-N4 | 132.5(1) |
| Fe2–N4 | 1.924(2) | N2-Fe2-N4 | 131.8(1) |
| Si1–N1 | 1.750(2) | Si1-O1-Si2 | 141.14(13) |
| Si2–N2 | 1.750(3) | | |

Unlike the $^1$H NMR of the iron(III) complexes, **5** gives relatively sharp peaks. The $^1$H NMR spectrum of **5** shows five shifted peaks assignable to the *tert*-butyl (−7.69 ppm), the silylmethyl groups (−0.66 ppm) and the *ortho*, *meta* and *para* protons (−15.62, 10.50, −5.61 ppm) of the -NPh$_2$ groups, respectively. The alternating shift pattern in the phenyl rings is a feature that is often observed in paramagnetic $^1$H NMR spectra. Note that in solution, the silylmethyl and *tert*-butyl protons in **5** are equivalent; thus, the silylether donor must be oscillating rapidly between the two iron centres in a fluxional process at room temperature, yielding an average signal.

The room temperature $\mu_{eff}$ value of 4.5 BM per iron for **5**, typical for high-spin iron(II), gradually decreases to 2.3 BM at 2 K, indicative of weak antiferromagnetic coupling between the two iron atoms (Figure 2); there is no maximum in the $\chi_M$ versus $T$ data and thus the very weak coupling was not modeled. Finally, the Mössbauer spectrum of **5** shows a doublet with an isomer shift typical of high spin iron(II) (Table 1).[26, 30, 34]

Reaction of **1** with LiPPh$_2$ instead of LiNPh$_2$ quantitatively yielded a different reduced product: the previously observed phosphorus-free amido-bridged dimeric iron(II) complex $\{Fe[t\text{BuN}(SiMe_2)]_2O\}_2$.[5] The identity of this product was confirmed by X-ray crystallography and by comparison with the sharp but paramagnetically shifted $^1$H NMR spectrum of an independently prepared sample of $\{Fe[tBuN(SiMe_2)]_2O\}_2$.

**Reactivity of the ate complexes**: Despite the presence of Li–π interactions, the ate complexes **2**–**4** also appear susceptible to halide metathesis. The reaction of ate-complex **2** with a variety of alkyllithium reagents (e.g. MeLi, $Me_3SiCH_2Li$) gave a change in colour from dark orange to dark red at low temperature, perhaps indicative of the formation of an iron(III)–alkyl. However, warming to room temperature resulted in reduction to the halide-free, amido-bridged dimeric iron(II) complex $\{Fe[Me_3PhN(SiMe_2)]_2O\}_2$ (**6**). This dimer was prepared independently by reaction of $FeCl_2$ with $\{Li_2[2,4,6\text{-}Me_3PhN(SiMe_2)]_2O\}$ for comparison. These metal systems are among the few that have been shown to be easily reduced when reacted with other σ-donor anions.[35] Further substitution chemistry of these complexes is under investigation.

A different redox reaction was observed to a much smaller degree as a competing side reaction in the initial synthesis of **2**–**4** from $FeX_3$ and the dilithiodiamido ligand, which increased with the electron-withdrawing character of the amide. Thus, no side product is observed in the synthesis of *t*Bu amido-substituted **1** and only small amounts for 2,4,6-$Me_3Ph$ or 2,6-$iPr_2Ph$ amido-substituted **2**–**4** are generated.[36] However, reaction of the electron-withdrawing diamidoether ligand $\{Li_2[3,5\text{-}(CF_3)_2PhN(SiMe_2)]_2O\}$[8] with $FeX_3$ resulted in complete reduction to iron(II) products, which were identified as THF adducts of $FeX_2$. Specifically, a linear one-dimensional chain of the form $[FeBr_2(THF)_2]_n$ (**7**) (Figure 5) was isolated from the $FeBr_3$-containing reaction (selected interatomic distances and bond angles are listed in Table 4). The iron atoms in **7** have a pseudo-octahedral geometry; each iron atom is coordinated to four bromine atoms and two THF molecules. The iron atoms of the chain are bridged by the bromine atoms with Fe–Br distances of 2.6754(4) and 2.6833(4) Å. In addition, $[Fe_4Cl_8(THF)_6]$[37] was isolated from the $FeCl_3$-containing reaction. Although lithium amides are known in the literature with regards to their ability to reduce organic molecules,[38] their reduction of metal halides has not been widely reported.

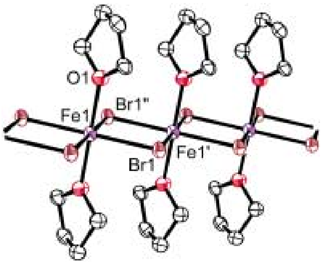

Figure 5. Chain structure of **7** (ORTEP view, 50 % probability ellipsoids are shown).

Table 4. Selected interatomic distances [Å] and bond angles [°] for $[FeBr_2(THF)_2]_n$ (**7**).

| | | | |
|---|---|---|---|
| Fe–Br1 | 2.6754(4) | Fe1–Fe1[i] | 3.981(1) |
| Fe–Br1[ii] | 2.6833(4) | Fe1[i]-Br1-Fe1 | 95.949(14) |
| Fe1–O1 | 2.133(3) | Br1-Fe1-Br1[ii] | 84.051(14) |

[i] $= -1+x, y$, z. [ii] $= -x, 1-y, 1-z$.

## Conclusion

Dimeric iron(III)–diamido complexes of the type $\{FeX_2\text{-}Li[RN(SiMe_2)]_2O\}_2$ were synthesized, giving rise to unusual transition metal ate complexes that are stabilized by Li–π interactions. These complexes are tetrahedral and high-spin in comparison with the five-coordinate spin admixed, *tert*-butyl system **1**. They are reactive in halide metathesis with other σ-donor anions, despite the presence of Li–π interactions but result in reduced iron(II) products. The reactivity of related diamidoether complexes is currently under investigation.

## Experimental Section

**General**: All experiments were carried out under an atmosphere of dry, oxygen-free dinitrogen by means of standard Schlenk or glovebox techniques. The glovebox used was a Mbraun Labmaster 130 equipped with a solvent purification system and a −35 °C freezer. Diethyl ether ($Et_2O$) and tetrahydrofuran (THF) were predried over sodium wire and were freshly distilled under a dinitrogen atmosphere by using sodium/benzophenone and potassium/benzophenone, respectively. Hexanes and toluene were passed through the solvent purification system connected to the glovebox. [$D_6$]Benzene was distilled from sodium benzophenone and stored under dinitrogen. $[tBuNH(SiMe_2)]_2O$,[5, 6, 12] $[2,4,6\text{-}Me_3PhNH(SiMe_2)]_2O$,[8] $[2,6\text{-}iPr_2PhNH(SiMe_2)]_2O$,[8] $[3,5\text{-}(CF_3)_2PhNH(SiMe_2)]_2O$,[8] $\{Fe[tBuN(SiMe_2)]_2O\}_2$[5] and $\{FeCl[tBuN(SiMe_2)]_2O\}_2$[12] were prepared as previously described. All other reagents were bought from commercial sources and used as received. The variable temperature magnetic susceptibility of crystalline samples were measured over the range 2–300 K and at a field of 10000 G using a Quantum Design (MPMS) SQUID magnetometer. The sample holder, made of PVC, was specifically designed to possess a constant cross-sectional area. UV/Vis spectra were recorded on a HP-8452A diode array spectrophotometer. $^1$H NMR Spectra were conducted on a 400 MHz Bruker AMX instrument. Mass Spectra were measured using a HP-5985 GC-MS EI/CI instrument operating at 70 eV. Elemental analysis (C, H, N) was conducted by Mr. Miki Yang of Simon Fraser University.

**$\{FeCl_2Li[Me_3PhN(SiMe_2)]_2O\}_2$ (2)**: A white powder of $[2,4,6\text{-}Me_3PhNH(SiMe_2)]_2O$ (0.5 g, 1.25 mmol) was dissolved in $Et_2O$ (20 mL) and two equivalents of 1.6 M *n*BuLi in hexanes (1.56 mL, 2.5 mmol) were added dropwise at −78 °C. After being stirred for 2 h at room temperature, the resulting solution was added dropwise to anhydrous $FeCl_3$ (0.2 g, 1.25 mmol) in $Et_2O$ (40 mL) at −78 °C, yielding a dark orange/red solution. After 2 h of being stirred at room temperature, the solvent was removed in vacuo, the residue was extracted in hexanes and filtered through Celite. Analytically pure product was obtained from refrigeration of this solution at −35 °C followed by collection of the resulting crystals (0.62 g, 80 %) on a fine frit. $^1$H NMR (400 MHz, $C_6D_6$, 25 °C): $\delta = 151$ (br), 135 (br), 28 (br); elemental analysis calcd (%) for $C_{22}H_{34}N_2Cl_2FeLiOSi_2$: C 49.63, H 6.44, N 5.26; found: C 49.50, H 6.77, N 4.88.

**$\{FeBr_2Li[Me_3PhN(SiMe_2)]_2O\}_2$ (3)**: A procedure analogous to the synthesis of **2** was used with $[2,4,6\text{-}Me_3PhNH(SiMe_2)]_2O$ (0.5 g, 1.25 mmol), 1.6 M *n*BuLi in hexanes (1.56 mL, 2.5 mmol) and anhydrous $FeBr_3$ (0.37 g, 1.25 mmol). Single crystals of **3** suitable for X-ray analysis were obtained from the slow evaporation of a hexanes solution (0.61 g, 69 %). $^1$H NMR (400 MHz, $C_6D_6$, 25 °C): $\delta = 152$ (br), 120 (br), 27 (br); elemental analysis calcd (%) for $C_{22}H_{34}N_2Br_2FeLiOSi_2$: C 42.53, H 5.52, N 4.51; found: C 42.19, H 5.61, N 4.27.

**$\{FeCl_2Li[iPr_2PhN(SiMe_2)]_2O\}_2$ (4)**: A procedure analogous to the synthesis of **2** (and **3**) was used with $[2,6\text{-}iPr_2PhNH(SiMe_2)]_2O$ (0.5 g, 1.03 mmol), 1.6 M *n*BuLi in hexanes (1.23 mL, 2.06 mmol) and anhydrous $FeCl_3$ (0.17 g, 1.03 mmol). Refrigeration of a hexanes solution at −35 °C gave dark crystals of **4** (0.64 g, 88 %). $^1H$ NMR (400 MHz, $C_6D_6$, 25 °C): $\delta = 119$ (br), 21 (br), −105 (br); elemental analysis calcd (%) for $C_{28}H_{46}N_2Cl_2FeLiOSi_2 \cdot C_6H_{14}$: C 58.11, H 8.61, N 3.98; found: C 58.19, H 8.54, N 3.89.

**{Fe$_2$(NPh$_2$)$_2$[*t*BuN(SiMe$_2$)]$_2$O} (5)**: The purple powder {FeCl[*t*BuN(SiMe$_2$)]$_2$O}$_2$ (**1**) (0.2 g, 0.27 mmol) was dissolved in $Et_2O$ (20 mL) and a solution of $LiNPh_2$ (0.096 g, 0.55 mmol) in $Et_2O$ (10 mL) was added dropwise at −78 °C. A dark violet colour developed upon warming to room temperature. After being stirred overnight at room temperature, the solvent was removed in vacuo, the product was extracted in hexanes and filtered through Celite. Slow evaporation of a hexanes solution yielded large block crystals of **5** (0.17 g, 87 %). $^1H$ NMR (400 MHz, $C_6D_6$, 25 °C): $\delta = 10.50$ (s, 8H; *m-Ph*), −0.66 (s, 12H; Si*Me$_2$*), −5.61 (s, 4H; *p-Ph*), −7.69 (s, 18H; C(*CH$_3$*)$_3$), −15.62 (s, 8H; *o-Ph*); MS (70 eV, CI): *m/z*: 723 [$M^+$], 552 [$M^+ - NPh_2$]; elemental analysis calcd (%) for $C_{36}H_{50}N_4Fe_2OSi_2$: C 59.83, H 6.97, N 7.75; found: C 59.70, H 6.73, N 7.78.

**{Fe[Me$_3$PhN(SiMe$_2$)]$_2$O}$_2$ (6)**: A white powder of [2,4,6-Me$_3$PhNH(SiMe$_2$)]$_2$O (0.71 g, 1.78 mmol) was dissolved in THF (20 mL) and two equivalents of 1.6 M *n*BuLi in hexanes (2.20 mL, 3.55 mmol) were added dropwise at −78 °C. After being stirred for 2 h at room temperature, the resulting solution was added dropwise to anhydrous $FeCl_2$ (0.225 g, 1.78 mmol) in $Et_2O$ (40 mL) at −78 °C, yielding a dark yellow solution. After 2 h of being stirred at room temperature, the solvent was removed in vacuo, the residue was extracted in toluene and filtered through Celite. A powder of **6** precipitated upon refrigeration of this solution at −35 °C, which was washed with hexanes (0.31 g, 40 %). $^1H$ NMR (400 MHz, $C_6D_6$, 25 °C): $\delta = 42$, 34, 30, 27, 22, 7.42, 2.27, 0.35, −21, −31, −50, −54; elemental analysis calcd (%) for $C_{22}H_{34}N_2FeOSi_2$: C 58.13, H 7.54, N 6.16; found: C 57.79, H 7.42, N 5.94.

**[FeBr$_2$(THF)$_2$]$_n$ (7)**: The dark brown oil [3,5-(CF$_3$)$_2$PhNH(SiMe$_2$)]$_2$O (1.0 g, 1.7 mmol) was dissolved in $Et_2O$ (20 mL) and two equivalents of 1.6 M *n*BuLi in hexanes (2.13 mL, 3.4 mmol) were added dropwise at −78 °C. After being stirred for 2 h at room temperature, the resulting solution was added dropwise to anhydrous $FeBr_3$ (0.50 g, 1.7 mmol) in $Et_2O$ (40 mL) at −78 °C, yielding a dark brown solution. After being stirred overnight at room temperature, the solvent was removed in vacuo, the residue was extracted in hexanes and filtered through Celite. Crystals of **7** suitable for X-ray analysis were obtained from refrigeration of a THF/hexanes solution at −35 °C. Elemental analysis calcd (%) for $C_8H_{16}Br_2FeO_2$: C 26.70, H 4.48; found: C 20.65, H 2.89. The poor analysis is likely due to the partial evaporation of THF.

**Reaction of 1 with LiPPh$_2$ to give {Fe[*t*BuN(SiMe$_2$)]$_2$O}$_2$**: The dark purple powder **1** (0.2 g, 0.55 mmol) was dissolved in $Et_2O$ (20 mL) whereupon a solution of $LiPPh_2$ (0.105 g, 0.55 mmol) in $Et_2O$ (10 mL) was added dropwise at −78 °C. An immediate colour change to dark brown/green occurred. After 2 h of being stirred at room temperature, the solvent was removed in vacuo, the residue was extracted in hexanes and filtered through Celite. Single crystals of {Fe[*t*BuN(SiMe$_2$)]$_2$O}$_2$ were grown from refrigeration of this solution at −35 °C (0.16 g, 89 %). $^1H$ NMR of independently prepared {Fe[*t*BuN(SiMe$_2$)]$_2$O}$_2$ gave the same NMR fingerprint. $^1H$ NMR (400 MHz, $C_6D_6$, 25 °C): $\delta = 15.58$ (s, 3H; Si*Me*), 10.57 (s, 3H; Si*Me*), 6.18 (s, 9H; C(*CH$_3$*)$_3$), 3.07 (s, 3H; Si*Me*), 2.72 (s, 3H; Si*Me*), 0.15 (s, 9H; C(*CH$_3$*)$_3$).

**Reaction of 2 with MeLi to give {Fe[Me$_3$PhN(SiMe$_2$)]$_2$O}$_2$ (6)**: An NMR tube was charged with the red/orange powder **2** (0.020 g, 0.056 mmol) and dissolved in [D$_8$]toluene (0.5 mL). To this was added 1.6 M MeLi in $Et_2O$ (0.07 mL, 0.11 mmol). The $^1H$ NMR spectrum of this sample gave the same NMR fingerprint as independently prepared **6**.

**X-ray crystallographic analyses of 3, 5, and 7**: See Table 5 for crystal data. Selected interatomic distances and bond angles for **3**, **5**, and **7** are found in Tables 2–4, respectively. Suitable crystals for **3**, **5**, and **7** were mounted in a capillary under $N_2$ (glovebox) and analyzed on the following instruments: For **3**, a P4 Bruker diffractometer equipped with a Bruker SMART 1 K CCD area detector (employing the program SMART)[39] and a rotating anode utilizing graphite-monochromated $Mo_{K\alpha}$ radiation ($\lambda = 0.71073$ Å). Data processing was carried out by use of the SAINT program,[40] while the program SADABS[41] was utilized for the scaling of diffraction data, the application of a decay correction and an empirical absorption correction based on redundant reflections. The structure of **3** was solved by using the direct-methods procedure in the Bruker SHELXTL program library[42] and refined by full-matrix least-squares methods on $F^2$. All non-hydrogen atoms were refined using anisotropic thermal parameters. For **5** and **7**, data was collected on a Enraf-Nonius CAD4 diffractometer. The programs used for all absorption corrections, data reduction and structure solutions of **5** and **7** were from the NRCVAX Crystal Structure System.[43] The structures were refined using CRYSTALS.[44] All diagrams were made using Ortep-3.[45]

Table 5. Crystal data for **3**, **5** and **7**.

| | **3** | **5** | **7** |
|---|---|---|---|
| empirical formula | $C_{44}H_{68}Br_4Fe_2Li_2N_4O_2Si_4$ | $C_{36}H_{50}Fe_2N_4OSi_2$ | $C_8H_{16}Br_2FeO_2$ |
| formula weight | 1242.60 | 722.69 | 359.87 |
| $T$ [K] | 153(2) | 293 | 293 |
| $\lambda$ [Å] | 0.71073 | 0.71073 | 0.71073 |
| crystal system | monoclinic | triclinic | monoclinic |
| space group | $P2_1/c$ | $P\bar{1}$ | $P2_1/n$ |
| $a$ [Å] | 16.887(7) | 10.4168(25) | 3.9807(7) |
| $b$ [Å] | 10.983(4) | 10.6957(20) | 7.5170(15) |
| $c$ [Å] | 15.899(5) | 17.467(3) | 18.262(4) |
| $\alpha$ [°] | 90.00 | 95.131(16) | 90.00 |
| $\beta$ [°] | 108.952(12) | 97.971(18) | 90.086(17) |
| $\gamma$ [°] | 90.00 | 100.711(17) | 90.00 |
| $V$ [Å$^3$] | 2789.1(17) | 1880.5(6) | 546.5(2) |
| $Z$ | 2 | 2 | 2 |
| $\rho_{calcd}$ [g cm$^{-3}$] | 1.480 | 1.277 | 2.187 |
| $\mu$ [mm$^{-1}$] | 3.51 | 0.87 | 8.59 |
| $F$(000) | 1260 | 766 | 352 |
| crystal size [mm$^3$] | 0.60 × 0.20 × 0.12 | 0.5 × 0.4 × 0.4 | 0.3 × 0.25 × 0.2 |
| $\theta$ range [°] | 2–27.54 | 2–25.06 | 2–29.06 |
| refls collected | 36744 | 7389 | 1575 |
| indep refls | 18354 | 6660 | 1464 |
| data/parameters | 18354/298 | 4386/409 | 1008/62 |
| $R$ indices [$I > x\sigma(I)$][a] | | | |
| $R(F^2)$ | 0.0495 | | |
| $wR(F^2)$ | 0.0979 | | |
| $R_F$ | | 0.0312 | 0.0358 |
| $R_{WF}$ | | 0.0330 | 0.0392 |

[a] ($x = 2$ for **3**, $x = 2.5$ for **5** and **7**).

For **7**, because the angle $\beta$ differed little from 90°, and the refined structure in $P2_1/n$ displays approximate *mmm* symmetry, the possibility that the crystal was actually orthorhombic was re-considered. $R_{merge} = 0.085$ for crystal point group *mmm* (681 equivalent observed reflections), whereas $R_{merge} = 0.033$ for crystal point group $2/m$ (231 equivalent observed reflections) using the same absorption-corrected data. In the space group *Pmnn*, the structure could be refined to $R_F = 0.037$, for 46 refined parameters and 624 observed reflections, using the merged data. In this model, possible disorder was evident in the very large $U_{11}$ for the C-atoms of the THF ligand (which all lie in the mirror plane at x = 0.5). The same level of agreement could be obtained using split isotropic carbon and hydrogen atom sites (39 refined parameters). On the other hand, in $P2_1/n$, the stable refinement ($R_F = 0.036$, for 62 refined parameters and 1008 observed reflections) produces a structure in which the puckering and packing of the THF ligands and the thermal motion of all atoms is most reasonable. Therefore, the $P2_1/n$ model is reported here, even though this assignment is not conclusive. Further investigation to resolve this possible ambiguity was considered unwarranted.

CCDC-198661 (**3**), -198662 (**5**) and -207311 (**7**) contain the supplementary crystallographic data (excluding structural factors) for this paper. These data can be obtained free of charge via www.ccdc.cam.ac.uk/conts/retrieving.html (or from the Cambridge Crystallographic Data Centre on application to CCDC, 12 Union Road, Cambridge CB2 1EZ, UK; fax: (+44)1223-336-033; or e-mail: deposit@ccdc.cam.ac.uk).

**Mössbauer analyses of 1–5**: The crystalline samples used for Mössbauer spectroscopy were loaded into teflon holders in a glovebox. Samples were stored in liquid nitrogen prior to spectra collection. The Mössbauer experiments were recorded using a Harwell Instruments constant acceleration drive coupled to a MSA 200 attenuator and a MWG 200 signal generator. The detector was a Reuter-Stokes Kr/CO$_2$ proportional counter and a 25 mCi $^{57}$Co/Rh source was used. Spectra were recorded at 77 and 4.2 K. The spectrometer was routinely calibrated using iron foil as the standard.

## Acknowledgement

D.B.L. is grateful to NSERC of Canada for support of this research.

---

[1] D. C. Bradley, M. H. Chisholm, *Acc. Chem. Res.* **1976**, *9*, 273.

[2] R. Kempe, *Angew. Chem.* **2000**, *112*, 478; *Angew. Chem. Int. Ed.* **2000**, *39*, 468.

[3] N. A. H. Male, M. Thornton-Pett, M. Bochmann, *J. Chem. Soc. Dalton Trans.* **1997**, 2487; M. Aizenberg, L. Turculet, W. M. Davis, F. Schattenmann, R. R. Schrock, *Organometallics* **1998**, *17*, 4795.

[4] J. D. Scollard, D. H. McConville, J. J. Vittal, *Organometallics* **1997**, *16*, 4415; F. G. N. Cloke, P. B. Hitchcock, J. B. Love, *J. Chem. Soc. Dalton Trans.* **1995**, 25; F. Guérin, D. H. McConville, N. C. Payne, *Organometallics* **1996**, *15*, 5085; L.-C. Liang, R. R. Schrock, W. M. Davis, D. H. McConville, *J. Am. Chem. Soc.* **1999**, *121*, 5797; D. D. Graf, R. R. Schrock, W. M. Davis, R. Stumpf, *Organometallics* **1999**, *18*, 843; R. Baumann, W. M. Davis, R. R. Schrock, *J. Am. Chem. Soc.* **1997**, *119*, 3830; L.-C. Liang, R. R. Schrock, W. M. Davis, *Organometallics* **2000**, *19*, 2526; L. H. Gade, *Chem. Commun.* **2000**, 173; H. Mack, M. S. Eisen, *J. Organomet. Chem.* **1996**, *525*, 81.

[5] A. J. Elias, H. W. Roesky, W. T. Robinson, G. M. Sheldrick, *J. Chem. Soc. Dalton Trans.* **1993**, 495.

[6] A. J. Elias, H.-G Schmidt, M. Noltemeyer, H. W. Roesky, *Eur. J. Solid State Inorg. Chem.* **1992**, *29*, 23.

[7] H. Ikeda, T. Monoi, Y. Nakayama, H. Yasuda, *J. Organomet. Chem.* **2002**, *642*, 156.

[8] G. Mund, A. J. Gabert, R. J. Batchelor, J. F. Britten, D. B. Leznoff, *Chem. Commun.* **2002**, 2990; D. B. Leznoff, G. Mund, K. C. Jantunen, P. H. Bhatia, A. J. Gabert, R. J. Batchelor, *J. Nucl. Sci. Technol.* Nov. **2002**, Supplement 3, 406.

[9] J. J. Ellison, P. P. Power, S. C. Shoner, *J. Am. Chem. Soc.* **1989**, *111*, 8044; R. A. Bartlett, P. P. Power, *J. Am. Chem. Soc.* **1987**, *109*, 7563; B. B. Murray, P. P. Power, *Inorg. Chem.* **1984**, *23*, 4584; D. C. Bradley, M. B. Hursthouse, *J. Chem. Soc. Chem. Commun.* **1972**, 872; D. C. Bradley, M. B. Hursthouse, P. F. Rodesiler, *Chem. Commun.* **1969**, 14; H. Chen, R. A. Bartlett, H. V. Rasika Dias, M. M. Olmstead, P. P. Power, *J. Am. Chem. Soc.* **1989**, *111*, 4338.

[10] M. B. Hursthouse, P. F. Rodesiler, *J. Chem. Soc. Dalton Trans.* **1972**, 2100.

[11] M. M. Olmstead, P. P. Power, S. C. Shoner, *Inorg. Chem.* **1991**, *30*, 2547.

[12] G. Mund, R. J. Batchelor, R. D. Sharma, C. H. W. Jones, D. B. Leznoff, *J. Chem. Soc. Dalton Trans.* **2002**, 136.

[13] T. Kauffmann, *Angew. Chem.* **1996**, *108*, 401; *Angew. Chem. Int. Ed. Engl.* **1996**, *35*, 386; S. S. Al-Juaid, C. Eaborn, P. B. Hitchcock, M. S. Hill, J. D. Smith, *Organometallics* **2000**, *19*, 3224; D. Evans, M. S. Hill, P. B. Hitchcock, *J. Chem. Soc. Dalton Trans.* **2003**, 570; R. Wyrwa, H. Goris, *Z. Anorg. Allg. Chem.* **1999**, *625*, 1904; H. Bönnemann, C. Krüger, Y-H. Tsay, *Angew. Chem.* **1976**, *88*, 51; *Angew. Chem. Int. Ed. Engl.* **1976**, *15*, 46; U. Siemeling, U. Vorfeld, B. Neumann, H.-G. Stammler, *Inorg. Chem.* **2000**, *39*, 5159; J. M. Smith, R. J. Lachicotte, K. A. Pittard, T. R. Cundari, G. Lukat-Rodgers, K. R. Rodgers, P. T. Holland, *J. Am. Chem. Soc.* **2001**, *123*, 9222.

[14] K. J. Thurlow, *Chemical Nomenclature*, Kluwer Academic, London, **1998**; J. E. Huheey, E. A. Keiter, R. L. Keiter, *Inorganic Chemistry: Principles of Structure and Reactivity*, 4th ed., HarperCollins, New York, **1993**.

[15] R. Kempe, H. Noss, T. Irrgang, *J. Organomet. Chem.* **2002**, *647*, 12.

[16] P. Roussel, N. W. Alcock, P. Scott, *Chem. Commun.* **1998**, 801.

[17] F. T. Edelmann, D. M. M. Freckmann, H. Schumann, *Chem. Rev.* **2002**, *102*, 1851; H. Schumann, J. A. Meese-Marktscheffel, L. Esser, *Chem. Rev.* **1995**, *95*, 865; F. T. Edelmann, *Angew. Chem.* **1995**, *107*, 2647; *Angew. Chem. Int. Ed. Engl.* **1995**, *34*, 2466; F. Neif, P. Riant, L. Ricard, P. Desmurs, D. Baudry-Barbier, *Eur. J. Inorg. Chem.* **1999**, *6*, 1041; O. Just, W. S. Rees. Jr, *Inorg. Chem.* **2001**, *40*, 1751; C. Qian, W. Nie, J. Sun, *J. Chem. Soc. Dalton Trans.* **1999**, 3283; W. J. Evans, D. G. Giarikos, M. A. Johnston, M. A. Greci, J. W. Ziller, *J. Chem. Soc. Dalton Trans.* **2002**, 520; M. F. Lappert, A. Singh, *J. Organomet. Chem.* **1982**, *239*, 133; M. D. Fryzuk, L. Jafarpour, F. M. Kerton, J. B. Love, B. O. Patrick, S. J. Rettig, *Organometallics* **2001**, *20*, 1387.

[18] C. J. Burns, D. L. Clark, R. J. Donohoe, P. B. Duval, B. L. Scott, C. Drew Tait, *Inorg. Chem.* **2000**, *39*, 5464.

[19] F. G. Kirchbauer, P.-M. Pellny, H. Sun, V. V. Burlakov, P. Arndt, W. Baumann, A. Spannenberg, U. Rosenthal, *Organometallics* **2001**, *20*, 5289; J. R. Hagadorn, J. Arnold, *Organometallics* **1996**, *15*, 984; R. W. Quan, G. C. Bazan, A. F. Kiely, W. P. Schaefer, J. E. Bercaw, *J. Am. Chem. Soc.* **1994**, *116*, 4489; F. A. Cotton, M. P. Diebold, W. J. Roth, *J. Am. Chem. Soc.* **1987**, *109*, 5506; S. Hao, J.-I. Song, P. Berno, S. Gambarotta, *Organometallics* **1994**, *13*, 1326.

[20] W. N. Setzer, P. V. R. Schleyer, *Adv. Organomet. Chem.* **1985**, *24*, 353; B. Schiemenz, P. P. Power, *Angew. Chem.* **1996**, *108*, 2288; *Angew. Chem. Int. Ed. Engl.* **1996**, *35*, 2150; S. Kurz, E. Hey-Hawkins, *Organometallics* **1992**, *11*, 2729; K. W. Hellmann, C. Galka, L. H. Gade, A. Steiner, D. S. Wright, T. Kottke, D. Stalke, *Chem. Commun.* **1998**, 549; K. Ruhlandt-Senge, J. J. Ellison, R. J. Wehmschulte, F. Pauer, P. P. Power, *J. Am. Chem. Soc.* **1993**, *115*, 11353; H. Chen, R. A. Bartlett, H. V. Rasika Dias, M. M. Olmstead, P. P. Power, *Inorg. Chem.* **1991**, *30*, 2487.

[21] M. D. Fryzuk, D. B. Leznoff, E. S. F. Ma, S. J. Rettig, V. G. Young, Jr., *Organometallics* **1998**, *17*, 2313.

[22] O. Kahn, *Molecular Magnetism*, VCH, New York, **1993**.

[23] S. L. Stokes, W. M. Davis, A. L. Odom, C. C. Cummins, *Organometallics* **1996**, *15*, 4521.

[24] S. Pohl, U. Bierbach, W. Saak, *Angew. Chem.* **1989**, *101*, 796; *Angew. Chem. Int. Ed. Engl.* **1989**, *28*, 776.

[25] S. Pohl, W. Saak, *Z. Anorg. Allg. Chem.* **1985**, *523*, 25; W. Saak, S. Pohl, *Z. Anorg. Allg. Chem.* **1987**, *552*, 186; S. M. Nelson in *Comprehensive Coordination Chemistry, Vol. 4* (Eds.: G. Wilkinson, R. D. Gillard, J. A. McCleverty), Pergamon Press, Oxford, **1987**, 217.

[26] N. N. Greenwood, T. C. Gibb, *Mössbauer Spectroscopy*, Chapman and Hall, London, **1971**.

[27] M. Atanasov, R. H. Potze, G. A. Sawatzky, *J. Solid State Chem.* **1995**, *119*, 380.

[28] W. Kaim, B. Schwederski, *Bioinorganic Chemistry: Inorganic Elements in the Chemistry of Life*, Wiley, Chichester, **1994**.

[29] C. A. Reed, F. Guiset, *J. Am. Chem. Soc.* **1996**, *118*, 3281; M. M. Maltempo, *J. Chem. Phys.* **1974**, *61*, 2540; S. Mitra, V. R. Marathe, R. Birdy, *Chem. Phys. Lett.* **1983**, *96*, 103; F. U. Axe, C. Flowers, G. H. Loew, A. Waleh, *J. Am. Chem. Soc.* **1989**, *111*, 7333; E. L. Bominaar, R. Block, *J. Chem. Phys.* **1991**, *95*, 6712.

[30] P. Gütlich, R. Link, A. Trautwein, *Mössbauer Spectroscopy and Transition Metal Chemistry*, Springer, **1978**.

[31] S. S. Sandhu, S. S. Tandon, T. S. Lobana, D. S. Bedi, *Inorg. Chim. Acta* **1985**, *104*, 81; J. M. Friedt, D. Petridis, J. P. Sanchez, R. Reschke, A. Trautwein, *Phys. Rev.* **1979**, *B19*, 360; W. M. Reiff, W. A. Baker Jr., N. E. Erickson, *J. Am. Chem. Soc.* **1968**, *90*, 4794; S. L Kessel, D. N. Hendrickson, *Inorg. Chem.* **1980**, *19*, 1883; S. L Kessel, R. M. Emberson, P. G. Debrunner, D. N. Hendrickson, *Inorg. Chem.* **1980**, *19*, 1170.

[32] P. R. Edwards, C. E. Johnson, *J. Chem. Phys.* **1968**, *49*, 211.

[33] B. J. Kennedy, K. S. Murray, P. R. Zwack, H. Homborg, W. Kalz, *Inorg. Chem.* **1986**, *25*, 2539; M. Hanack, U. Keppeler, A. Lange, A. Hirsch, R. Dieing, in *Phthalocyanines: Properties and Applications, Vol. 2* (Eds.: C. C. Leznoff, A. B. P. Lever), VCH, New York, **1993**.

[34] D. J. Evans, *Chem. Phys. Lett.* **1996**, *255*, 134; C. D. Burbridge, D. M. L. Goodgame, *J. Chem. Soc (A)* **1968**, 1074.

[35] S. C. Dunn, P. Mountford, O. V. Shishkin, *Inorg. Chem.* **1996**, *35*, 1006; J. Chen, L. K. Woo, *Inorg. Chem.* **1998**, *37*, 3269; E. Hey-Hawkins, K. Fromm, *Polyhedron* **1995**, *14*, 2027.

[36] All physical and spectroscopic measurements of **2–4** were conducted on pure, recrystallized samples which were free of any iron(II) impurities.

[37] H. Zhao, R. Clérac, J.-S. Sun, X. Ouyang, J. M. Clemente-Juan, C. J. Gómez-García, E. Coronado, K. R. Dunbar, *J. Solid State Chem.* **2001**, *159*, 281; V. K. Bel'skii, V. M. Ishchenko, B. M. Bulychev, A. N. Protskii, G. L. Soloveichik, O. G. Ellert, Z. M. Seifulina, Y. V. Rakitin, V. M. Novotortsev, *Inorg. Chim. Acta* **1985**, *96*, 123; F. A. Cotton, R. L. Luck, K.-A. Son, *Inorg. Chim. Acta* **1991**, *179*, 11.

[38] K. Takeda, Y. Ohnishi, T. Koizumi, *Org. Lett.* **1999**, *1*, 237; E. P. Woo, K. T. Mak, *Tetrahedron Lett.* **1974**, *47*, 4095; U. Melamed, B.-A. Feit, *J. Chem. Soc. Perkin Trans. 1.* **1980**, 1267; G. F. Meijs, *J. Org. Chem.* **1987**, *52*, 3923; G. F. Meijs, *Tetrahedron Lett.* **1985**, *26*, 105.

[39] G. M. Sheldrick, SMART, version 4.05, Siemens Energy and Automation Inc., Madison, WI, 53719, **1996**.

[40] G. M. Sheldrick, SAINT, version 4.05, Siemens Energy and Automation Inc., Madison, WI, 53719, **1996**.

[41] G. M. Sheldrick, SADABS (Siemens Area Detector Absorption Corrections); Siemens Energy and Automation Inc., Madison, WI, 53719, **1996**.

[42] G. M. Sheldrick, SHELXTL, version 5.03, Siemens Crystallographic Research Systems, Madison, WI, **1994**.

[43] E. J. Gabe, Y. LePage, J.-P, Charland, F. L. Lee, P. S. White, *J. Appl. Crystallogr.* **1989**, *22*, 384.

[44] D. J. Watkin, C. K. Prout, J. R. Carruthers, P. W. Betteridge, R. I. Cooper, CRYSTALS Issue 11, Chemical Crystallography Laboratory, University of Oxford, Oxford (UK), **1999**.

[45] L. J. Farrugia, *J. Appl. Crystallogr.* **1997**, 30, 565.

Received: April 4, 2003 [F5014]